# Advanced Usage of the Software-Controlled Sensor Coupling Test

**H. Vallen**

**Abstract** By pulsing an acoustic emission (AE) sensor, AE of reproducible energy is artificially generated and used for the sensor coupling test. AE waves may travel from any AE source to a receiving AE sensor over multiple wave paths, e.g., over the shell or the liquid content of a pressure vessel. Waveform data may reveal different wave arrivals by so-called sub-events. Each wave arrival appears in waveform data by sub-events of different properties like arrival time, amplitude, frequency spectrum, and appearance of its envelope. Intelligent data processing software could automatically consider different wave propagation paths of an individual test object. This may answer questions like "did the wave of an individual sub-event propagate over the shell or over the liquid content of a pressure vessel?" and consider the right travel path and wave velocity for location calculation. By this, AE testing results could become in general more reliable. This chapter describes some basic work towards that objective. Development of such software would need feedback of waveform data from the sensor coupling check from real test objects.

## 1 Basics of the Software-Controlled Sensor Coupling Test

The original purpose of the software-controlled sensor coupling test was to offer the possibility that any channel can be selected by software to emit stimulated AE into a test object and to receive the resulting AE wave at the position of neighbored sensors. Each receiving sensor converts the wave to an electrical AE signal which is converted to digital AE data by an AE signal processor as usual (Fig. 1).

H. Vallen (✉)
Vallen Systeme GmbH, 82057 Icking, Germany
e-mail: hartmut@vallen.de

 
G. Shen et al. (eds.), *Advances in Acoustic Emission Technology*, Springer Proceedings in Physics 179, DOI 10.1007/978-3-319-29052-2_2

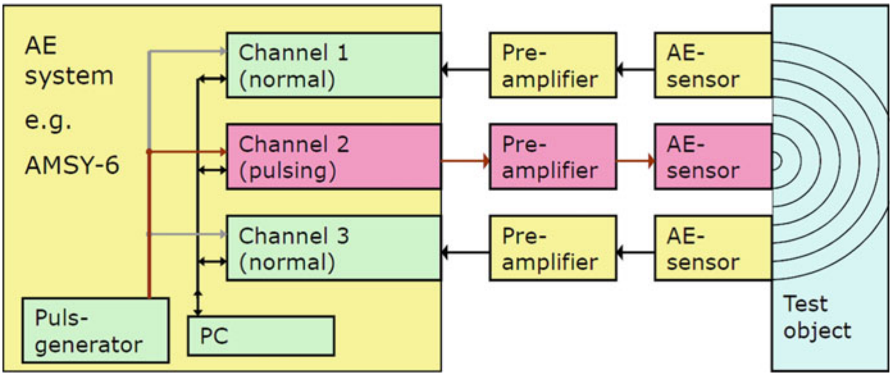


**Fig. 1** Block diagram of the "pulse-through" mechanism for the software-controlled sensor coupling test

## *1.1 Pulse-Through Principle*

In a so-called pulsing sequence, one channel is set to pulsing mode. That means, a few electrical pulses from a central pulse generator are passed through the channel up to the piezoelectric element. This causes one artificial AE event per pulse. Then the next channel is selected for pulsing until the last channel completes the pulsing sequence.

In "pulse-through mode" a programmable pulse amplitude in range 1 V–450 $V_{PP}$ can be used. The high amplitude maximum allows to receive pulses even over a very attenuating wave propagating path, e.g., through a polymer-layered riser tube. In pulsing mode, the preamplifier is switched off and the pulse is passed through up to the piezoelectric element over relay contacts. Each pulse is also fed into the signal processor in order to generate a hit data set with accurate time of the pulse. All data shown in this chapter are created by the pulse-through principle. Chapters 2 and 3 are included for completeness only.

## *1.2 Auto Sensor Test in Self-Test Mode*

This mode is defined by [1]: An electrical pulse is generated inside of a preamplifier in response to a control pulse on the 28 V power/signal line from the signal processor. The pulse is passed on to the piezoelectric element. The pulse amplitude can be modified in a small range by modifying the width of the control pulse. The preamplifier stays in operation and is driven into saturation by the pulse. After some settling time the preamplifier becomes able to receive an acoustic response from the test object. Under favorable circumstances, a change of coupling quality can be evaluated from the response on the emitted AE wave.

## 1.3 Auto Sensor Test in Near-Neighbor Mode

This mode is defined by [2]. A pulsing sequence is generated similar to the pulse-through principle described in Sect. 1.1 above, but the pulse is generated inside the preamplifier as with self-test mode described in Sect. 1.2. The pulse drives the preamplifier of the pulsing channel into saturation.

## 1.4 Pulsing Table

The amplitudes received during a pulsing sequence are shown in a pulsing table; see example of a six-channel configuration in Fig. 2. Lines are headed by the pulsing channel number, and columns by receiving channel numbers. Each cell shows the average of the few amplitudes (pulses) measured by a receiving channel. Non-plausible sensor responses can easily be identified. One of multiple pulsing sequences can be addressed by its tab on top of the table.

In addition, a variant of the pulsing table shows differences in amplitudes of two pulsing sequences, e.g., one before and the other after a test. This variant helps to quickly see whether acoustic coupling was constant before and after a test or has changed between any sensor pair.

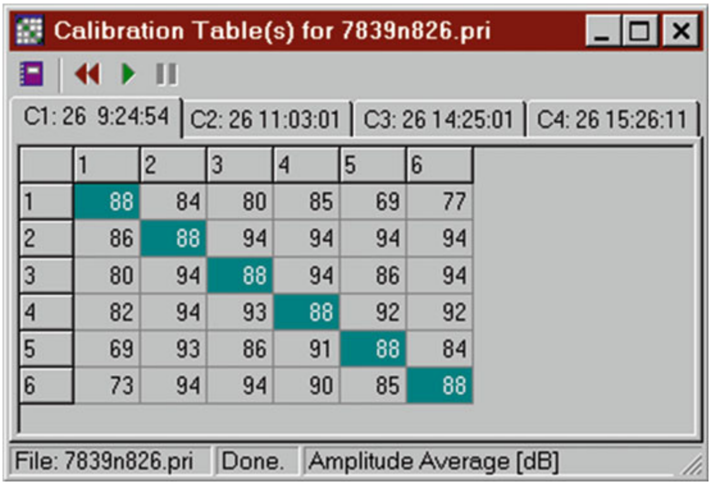


**Fig. 2** Pulsing table for a six-channel configuration. Channel 1 received 82 $dB_{AE}$ from pulsing channel 4

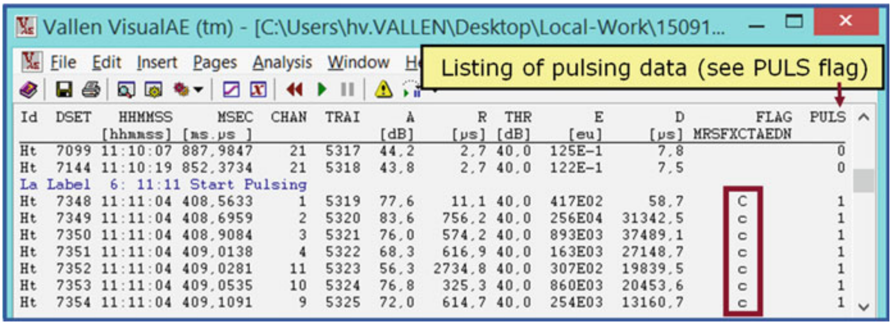


**Fig. 3** Example of a listing showing normal hit data ("PULS = 0"in last column) and the beginning of stimulated data ("PULS = 1"). The upper-case "C"-Flag in the listing identifies the pulse-emitting channel, the lower-case "c"-flag identifies pulse-receiving channels

## 2 Further Usage of Stimulated Pulsing Data

Stimulated AE data from pulsing sequences can be analyzed and graphically and numerically presented like normal AE data, e.g., for checking location calculation, clustering, attenuation profiles, and more (see Fig. 3).

Stimulated AE data from pulsing sequences can be separated from normal AE data by a filter condition: "PULS > 0." The "PULS" flag is selectable from the "Parametric results" dialog. The PULS Flag is set to 1 before the first channel is set to pulsing mode and back to 0 after the last channel is set from pulsing mode to normal mode.

## 3 Advanced Usage of the Software-Controlled Sensor Coupling Test

After looking at sensor coupling test data obtained from a few test objects, we discovered potential for an advanced, beneficial usage of those kind of data. Figure 4 shows an example with different wave arrivals in one data set.

The software-controlled sensor coupling test always generates AE at a well-defined position, namely the position of the pulsing sensor and at an accurate source time, which is measured as arrival time by the pulsing channel. From the position of each sensor, the distances of different propagation paths between each pair of sensors can be calculated. With a cylindric structure, most important propagation paths are the shortest and the next longer distance over the surface of the test object, and the shortest distance over the pressurization fluid in the test object. See the three paths from S1 to S2 in Fig. 5.

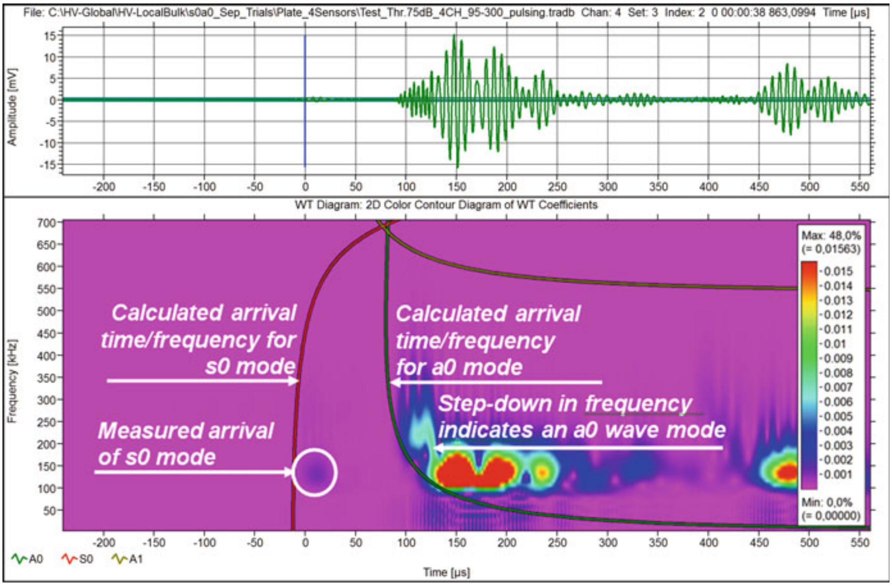


**Fig. 4** Data of a pulse-stimulated event from a plate. Since the sensor positions and the distance between pulse-transmitting and -receiving sensors are known, curves for the arrival time of each wave mode can be calculated from dispersion curves and shown in a time-scaled diagram relative to the first threshold crossing time

**Fig. 5** Shorter and longer paths between two sensors around a cylinder and over the liquid

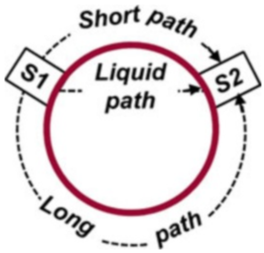


## 3.1 *Example 1: Thin-Walled Water-Filled Cylinder*

Outer diameter of cylinder: 125 cm, height of cylinder (without end caps): 120 cm, wall thickness of cylinder: 0.63 cm,

A program has been written to calculate the three distances (see Fig. 5) between any two positions on a cylinder and the resulting arrival times using a defined velocity of sound for each path (Fig. 6). The following abbreviations were used for the entered velocities, distances, and arrival times; the numbers are results for one example of positions S1 and S2:

| Entered velocities and positions S1(X1, Y1) and S2(X2, Y2): | | |
|---|---|---|
| svel= | 0.50 cm/µs | s0-velocity |
| avel= | 0.32 cm/µs | a0-velocity |
| waterv= | 0.15 cm/µs | Water velocity |
| X1= | 148 cm | Circumferential position of the source (range −196.35 ... +196.35) |
| Y1= | −25 cm | Height position of source (vertical cylinder) |
| X2= | −130 cm | Circumferential position of sensor 8 |
| Y2= | −130 cm | Height position of sensor 8 |

| Calculated distances: | | |
|---|---|---|
| Degree= | 105.15° | Angle between S1 and S2 (for water distance calculation) |
| surfDists= | 115 cm | Shortest surface distance |
| surfDistl= | 278 cm | Longer surface distance |
| volDist= | 99.6 cm | Water path distance |

| Calculated arrival times: | | |
|---|---|---|
| s0_short= | 230 µs | Delta-t of source to s0 arrival, refers to $T = 0$ |
| d_a0_short= | 129 µs | Short path a0-arrival from $T = 0$ |
| d_s0_long= | 326 µs | Long path s0-arrival from $T = 0$ |
| d_a0_long= | 639 µs | Long path a0-arrival from $T = 0$ |
| d_water= | 434 µs | Water path arrival from $T = 0$ |

### 3.2 *Example 2: Thick-Walled Water-Filled Cylinder*

| Dimensions | | No. of channels used: 50 |
|---|---|---|
| Length | 42.61 m | 40 at shell |
| Diameter | 5.48 m, | 3 at top head |
| Thickness (shell) | 14.5 cm | 7 at bottom head |

We received only a part of the test data (see Figs. 7, 8, and 9). Only stimulated data from sensors 1 to 4 are available, with 2048 samples at 5 Mega samples per second (MSPS) record length and 200 samples pre-trigger, that gives a visible length of 40 µs pre-trigger and 370 µs post-trigger. See Fig. 10.

Figure 10 shows a waveform picked up by sensor 42, emitted by pulse-stimulated sensor 3. The large-amplitude burst beginning at about 275 µs fits very well to the velocity of the Rayleigh wave.

Figure 11 shows same waveform as Fig. 10 but zoomed around the time of the first threshold crossing (FTC) (also called arrival time). Obviously, first components of the wave arrived about 25 µs before the measured arrival time. That means at such a thick-walled structure, the arrival time measurement bears some uncertainties. The question comes up, whether the peak time gives a more reliable time criterion for distance evaluation and location calculation than the arrival time.

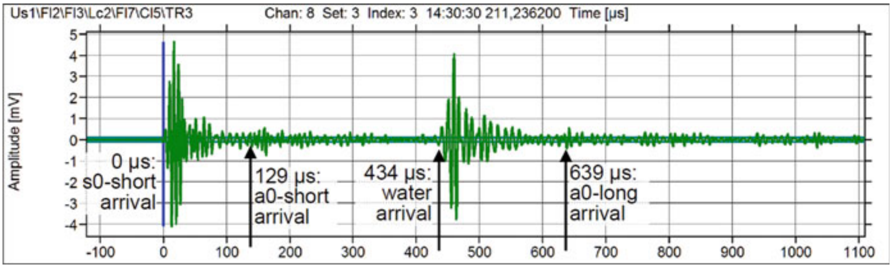


**Fig. 6** AE event generated by a pencil lead break (PLB) at position S1. Waveform received by sensor 8 at position S2. *Arrows* point to calculated arrival times. The water path arrival is very accurate; the s0-long arrival (at 326 µs) can't be identified in the waveform

**Fig. 7** Thick-walled cylinder

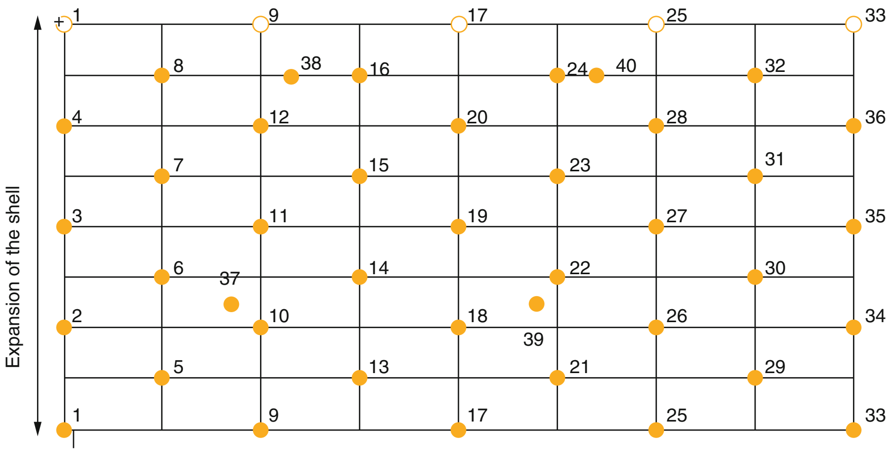


**Fig. 8** Sensor positions at (unwrapped) cylindrical part of pressure vessel

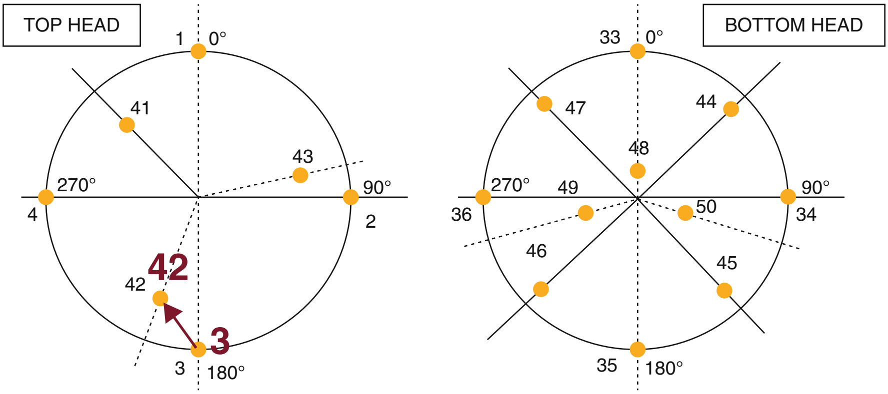


**Fig. 9** Sensor positions at top head (*left side*) and bottom head (*right side*). Four sensors belong to cylindrical part. Only distance between channels 3 and 42 (and 2 and 43) is short enough to see the Rayleigh wave arrival in the waveform data

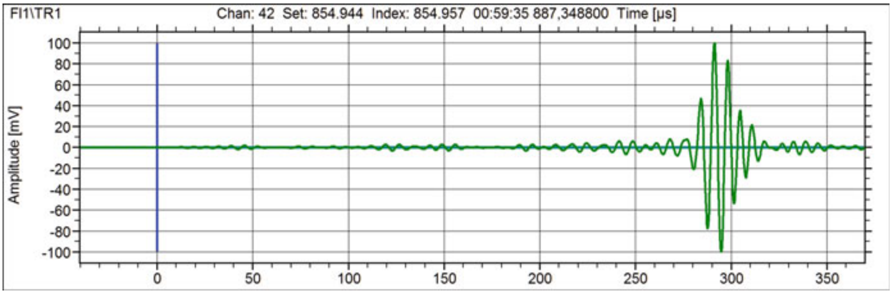


**Fig. 10** AE stimulated by sensor 3 and recorded by sensor 42

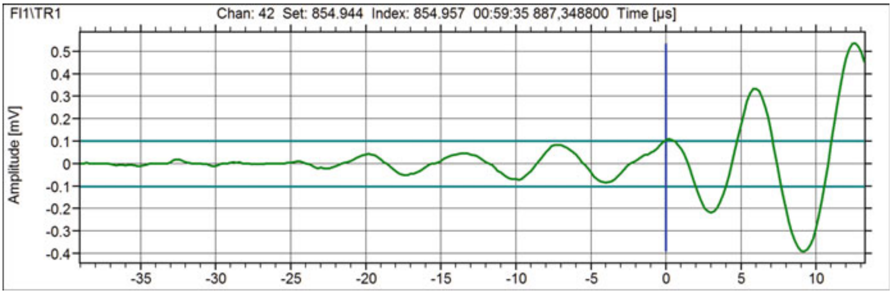


**Fig. 11** Waveform shown in Fig. 10 zoomed around first threshold crossing

The first four columns of the following table are taken from the listing of the channel 3-stimulated event. It shows:

| | |
|---|---|
| CHAN | Sensor number |
| DT1X | The difference between the measured arrival time of each subsequently hit channel to that of the FHC (channel 3) |
| *A* | The highest amplitude (peak amplitude) detected during the hit in $dB_{AE}$ |
| *R* | The rise time, defined as time of A minus arrival time (FTC time) |

The next columns show following calculated results:

| | |
|---|---|
| PkT | Peak time or time of *A*, the time at which the highest amplitude is measured, =DT1X + *R* |
| Dist_DT | Distance derived from arrival time, =DT1X × arrival time velocity (AV, 5.58 m/ms) |
| Dist_PKT | Distance derived from peak time, =PkT × peak time velocity (PV, 2.95 m/ms) |
| Deviation_in_% | The deviation of both distances in percent, =(Dist_DT/Dist_PKT) − 1) × 100 |

A positive deviation usually means that the delta-t (DT1X) is too large. The plausible effect can be derived from Fig. 11. Fast wave components are attenuated below threshold, so the arrival time later, when more energetic wave components arrive. This explains the occurrence of larger positive deviations at distances above 4.7 m (Table 1).

A negative deviation usually means that the peak time is detected too late. This can be seen with channels 6 and 7. There the rise time is a bit larger than at channels

**Table 1** Listing of subsequent hits of a stimulated event

| CHAN | DT1X (µs) | *A* (dB) | *R* (µs) | PkT (µs) | Dist_DT (m) | Dist_PkT (m) | Dist_DT/ Dist_PkT – 1 (%) |
|---|---|---|---|---|---|---|---|
| 3 | | 81.0 | 10.6 | | | | |
| 42 | 331.1 | 99.9 | 291.2 | 622.3 | 1.848 | 1.836 | 0.64 |
| 6 | 743.6 | 99.9 | 717.6 | 1461.2 | 4.149 | 4.311 | −3.74 |
| 7 | 759.2 | 99.4 | 726.4 | 1485.6 | 4.236 | 4.383 | −3.34 |
| 2 | 770.9 | 99.9 | 680.8 | 1451.7 | 4.302 | 4.283 | 0.45 |
| 4 | 771.3 | 99.9 | 674.2 | 1445.5 | 4.304 | 4.264 | 0.93 |
| 43 | 906.7 | 99.8 | 692.0 | 1598.7 | 5.059 | 4.716 | 7.28 |
| 41 | 1.139.8 | 99.9 | 854.4 | 1994.2 | 6.360 | 5.883 | 8.11 |
| 37 | 1.215.1 | 97.2 | 1.100.4 | 2315.5 | 6.780 | 6.831 | −0.74 |
| 11 | 1.339.6 | 96.0 | 1.203.6 | 2543.2 | 7.475 | 7.502 | −0.37 |
| 8 | 1.374.6 | 99.4 | 1.130.8 | 2505.4 | 7.670 | 7.391 | 3.78 |
| 5 | 1.391.1 | 98.7 | 1.145.6 | 2536.7 | 7.762 | 7.483 | 3.73 |
| 12 | 1.554.5 | 94.5 | 1.357.2 | 2911.7 | 8.674 | 8.590 | 0.98 |
| 10 | 1.570.6 | 93.8 | 1.367.6 | 2938.2 | 8.764 | 8.668 | 1.11 |
| 1 | 1.642.5 | 99.9 | 1.210.0 | 2852.5 | 9.165 | 8.415 | 8.92 |
| 38 | 1.921.6 | 92.3 | 1.576.8 | 3498.4 | 10.723 | 10.320 | 3.90 |
| 14 | 2.106.5 | 86.6 | 1.788.8 | 3895.3 | 11.754 | 11.491 | 2.29 |
| 9 | 2.139.2 | 92.7 | 1.711.2 | 3850.4 | 11.937 | 11.359 | 5.09 |

2 and 4. We could not look deeper into this phenomenon since the peak time is behind the recorded waveform length.

Since there are only very few occurrences of small negative deviations, we believe a peak-time-derived delta-t will lead to better location results than the arrival time delta-t, if the wall thickness is large and the AE source is at the outer surface of the object.

## 4 Conclusion

With two examples, a thin-walled and a thick-walled test object, this chapter shows that waveform data from the software-controlled sensor coupling test bear valuable information about details of wave propagation at the test object which might be helpful for the understanding of the involved wave propagation effects.

We would like to perform more studies on stimulated data from real test objects in order to define goals for the development of software that extracts most helpful information from such stimulated data. Substantial efforts are needed to equip a large structure with AE sensors for a properly performed AE test. It is very easy and needs almost no extra efforts to gather waveform data in addition to hit data during the automated sensor coupling test.

We herewith ask AE service providers to switch on waveform recording (TR recording) during the automatic sensor coupling test, use several ms long waveform length and about 1 ms pre-trigger setting, and pass on to us such data for further analysis. We will treat such data confidentially and eliminate any hint to the test object.

## References

1. ASTM E2374-10 "*Standard Guide for Acoustic Emission System Performance Verification*," Section 5.1.3.2. ASTM International, West Conshocken, PA, service@astm.org, www.astm.org
2. ASTM E2374-10 "*Standard Guide for Acoustic Emission System Performance Verification*," Section 5.1.3.1. ASTM International, West Conshocken, PA, service@astm.org, www.astm.org

Springer

http://www.springer.com/978-3-319-29050-8

Advances in Acoustic Emission Technology
Proceedings of the World Conference on Acoustic Emission–2015
Shen, G.; Wu, Z.; Zhang, J. (Eds.)
2017, XIV, 428 p. 309 illus., 267 illus. in color., Hardcover
ISBN: 978-3-319-29050-8